The Zipf distribution is an unambiguous target that any empirically accurate theory of the firm must hit. This result, taken together with those in (*21*) and (*27*), place important limits on models of firm dynamics. That is, (i) firm growth rates follow a Laplace distribution, (ii) the standard deviation in growth rates falls with initial firm size according to a power law, and (iii) large firms pay higher wages for the same job according to yet another power law (the so-called wage-size effect). Because the Zipf distribution obtains all the way down to the smallest sizes, it should be possible to derive Kesten-type processes and, hence, the Zipf distribution from a microeconomic model in which individual agents interact to form productive teams. Although today no analytically tractable models of this type exist, agent-based computational results have achieved significant success according to these criteria (*28*).

The Zipf distribution may describe firm sizes in other countries as well, a conjecture that can only be tested once individual governments make available—and in some cases gather for the first time—data that purport to be comprehensive.

**References and Notes**


1. Y. Ijiri, H. A. Simon, *Skew Distributions and the Sizes of Business Firms* (North-Holland, New York, 1977).
2. R. Gibrat, *Les Inégalitiés Économiques; Applications: aux inégalitiés des richesses, à la concentration des entreprises, aux populations des villes, aux statistiques des familles, etc., d'une loi nouvelle, la loi de l'effet proportionnel* (Librarie du Recueil Sirey, Paris, 1931).
3. J. Sutton, *J. Econ. Lit.* **XXXV**, 40 (1997).
4. G. K. Zipf, *Human Behavior and the Principle of Least Effort* (Addison-Wesley, Reading, MA, 1949).
5. J. Steindl, *Random Processes and the Growth of Firms* (Hafner, New York, 1965).
6. N. L. Johnson, S. Kotz, N. Balakrishnan, *Continuous Univariate Distributions* (Wiley, New York, ed. 2, 1994).
7. J. J. Ramsden, G. Kiss-Haypál, *Physica A* **277**, 220 (2000), who use a functional form slightly different from (*1*).
8. Although any finite sample will have moments, by definition, the nonexistence of moments in the context of real data implies that the moments give no indication of convergence as the number of data increase.
9. M. S. Watanabe, *Phys. Rev. E* **53**, 4187 (1996).
10. J. D. Burgos, P. Moreno-Tovar, *Biosystems* **39**, 227 (1996).
11. M. Gell-Mann, *The Quark and the Jaguar* (Freeman, New York, 1994), pp. 92–97.
12. L. Breslau *et al.*, *Proceedings of INFOCOM '99*, 21 to 25 March 1999, New York (IEEE Press, Piscataway, NJ, 1999), vol. 1, pp. 126–134.
13. M. H. R. Stanley *et al.*, *Econ. Lett.* **49**, 453 (1995).
14. Census data is based on Small Business Administration (SBA) tabulations; available at www.sba.gov/advo/stats/data.html.
15. Z. Acs, D. Audretsch, *Innovation and Small Firms* (MIT Press, Cambridge, MA, 1990).
16. Z. Acs, Ed., *Are Small Firms Important? Their Role and Impact* (Kluwer Academic, Boston, 1999).
17. M. Marsili, Y.-C. Zhang, *Phys. Rev. Lett.* **80**, 2741 (1998).
18. H. Takayasu, K. Okuyama, *Fractals* **6**, 67 (1998).
19. P. E. Hart, S. J. Prais, *J. R. Stat. Soc. Ser. A* **119**, 150 (1956).
20. P. E. Hart, N. Oulton, *Econ. J.* **106**, 1242 (1996).
21. M. H. R. Stanley *et al.*, *Nature* **379**, 804 (1996).
22. L. A. N. Amaral *et al.*, *J. Phys. I France* **7**, 621 (1997).
23. H. Kesten, *Acta Mathematica* **131**, 207 (1973).
24. O. Biham, O. Malcai, M. Levy, S. Solomon, *Phys. Rev. E* **58**, 1352 (1998).
25. X. Gabaix, *Q. J. Econ.* **CXIV**, 739 (1999).
26. O. Malcai, O. Biham, S. Solomon, *Phys. Rev. E* **60**, 1299 (1999).
27. C. Brown, J. Medoff, *J. Pol. Econ.* **97**, 1027 (1989).
28. R. L. Axtell, in preparation; available at www.brookings/edu/dynamics/papers/firms.

29. The Census data were gathered in March of 1997. Firms that had receipts during 1997 but no employees as of March are shown in the size 0 category. Such firms should be in one of the other size classes. One might assume that it is possible to adjust the data by including these firms in the overall distribution by having them follow the Zipf distribution, for instance. However, any such procedure leads to the unrealistic conclusion that some of these temporarily size 0 firms actually have thousands or tens of thousands of employees. The firms in the size 0 category in COMPUSTAT are ostensibly holding companies.
30. These data were created by the U.S. Census Bureau under contract to the Brookings Institution. Given that the bins are not equally sized, construction of the probability mass function shown in Fig. 1 proceeds by taking the number of firms in each bin and dividing by the width of the bin. The resulting adjusted frequency is then located at the geometric mean of the bin endpoints. The tail CDF shown in Fig. 2 was constructed by cumulating the raw population data.
31. The late H. A. Simon initiated my interest in this subject. Lectures on Zipf's law by M. Gell-Mann at the Santa Fe Institute and conversations with B. Mandelbrot, B. Morel, and P. Bak were formative in my thinking. I thank Z. Acs, T. Åstebro, W. Dickens, C. Graham, J. Lanjouw, F. Pryor, J. Roth, and H. P. Young for suggestions, and T. Cole, R. Constantino, R. Hammond, and K. Landis for assistance. Support from the National Science Foundation, the Alex C. Walker Foundation, and the John D. and Catherine T. MacArthur Foundation is gratefully acknowledged.

30 April 2001; accepted 9 August 2001

# Segregation of Human Neural Stem Cells in the Developing Primate Forebrain

**Václav Ourednik,[1]*† Jitka Ourednik,[1]* Jonathan D. Flax,[1] W. Michael Zawada,[2] Cynthia Hutt,[2] Chunhua Yang,[1] Kook I. Park,[1,3] Seung U. Kim,[4] Richard L. Sidman,[5] Curt R. Freed,[2]‡ Evan Y. Snyder[1]†‡**

**Many central nervous system regions at all stages of life contain neural stem cells (NSCs). We explored how these disparate NSC pools might emerge. A traceable clone of human NSCs was implanted intraventricularly to allow its integration into cerebral germinal zones of Old World monkey fetuses. The NSCs distributed into two subpopulations: One contributed to corticogenesis by migrating along radial glia to temporally appropriate layers of the cortical plate and differentiating into lamina-appropriate neurons or glia; the other remained undifferentiated and contributed to a secondary germinal zone (the subventricular zone) with occasional members interspersed throughout brain parenchyma. An early neurogenetic program allocates the progeny of NSCs either immediately for organogenesis or to undifferentiated pools for later use in the "postdevelopmental" brain.**

As cells with stemlike qualities have come to be identified within a widening range of organs [e.g., (*1*, *2*)], new questions have arisen about their relevance to normal development. The central nervous system (CNS) may serve as a bellwether for insights in this field. NSCs have been identified in the mammalian CNS, including humans (*3*–*9*), at stages from fetus to adult in a surprisingly wide range of regions (*10*–*13*). NSCs, defined as self-renewing, propagatable primordial cells each with the capacity to give rise to differentiated progeny within all neural lineages in all regions of the neuraxis, are posited to exist in the embryonic and fetal ventricular germinal zone (VZ) where they participate in CNS organogenesis (*5*, *14*, *15*). Cells equally "stemlike" in their potential have been identified at later stages (including old age) from a variety of regions: subventricular (SVZ) (*13*–*17*) and ependymal (*18*) zones of the forebrain, subgranular zone of the hippocampus (*6*–*10*, *19*), retina (*20*) and optic nerve (*10*, *11*), cerebellum (*12*), spinal cord (*21*), and even cortical parenchyma (*10*, *15*, *22*). How might these observations be reconciled? Are such stemlike pools, particularly those isolated from various parenchymal regions at "postdevelopmental" periods, of physiological relevance or artifacts of experimental manipulation (*10*, *11*)? Do these populations represent the same lineage or unique pools (*17*)? Of what relevance are these cells to normal human CNS development and repair?

We hypothesized that multiple stem cell pools, descendants of a common NSC, emerge during early cerebrogenesis as cells are used in organogenesis and concurrently

also set aside to establish a reservoir for subsequent use in homeostasis and repair. This could represent a developmental strategy in which plasticity is programmed into the CNS at the single-cell level from early stages of embryogenesis.

We sought to determine how progeny of a single traceable clone of NSCs get segregated during development by using a system that might also lend insight into human development. We grafted a clone of NSCs of human derivation (*5*, *23*) into the developing brains of fetal bonnet monkeys (*Macaca radiata*), an Old World species (Web note 1) (*24*). We asked what the fate would be of human cells transplanted at a time when neocortical cell genesis, migration, and differentiation are intensive (*25*–*27*). The primate neocortex, at the appropriate developmental stage, allows a distinction between layers of active neuron birth and layers where neurogenesis has been completed and glial cells are instead acquired (*27*) (Web note 2) (*24*) (Fig. 1, schematics I and II). One can discern experimentally the responses to local developmental cues simply by assaying the spatial segregation and patterns of differentiation of NSCs of a single clone in a given animal's brain after a single transplantation procedure. [A summary of simian cortical development is provided in an expanded legend to Fig. 1 in Web note 2 (*24*)]. Under transabdominal ultrasonic guidance, bonnet monkey fetuses at 12 to 13 weeks gestation received a single in utero injection of $\sim 2 \times 10^7$ clonally related undifferentiated NSCs [prelabeled with the nuclear marker 5-bromo-2′-deoxyuridine (BrdU)] into the left lateral cerebral ventricle, allowing the cells access to the VZ from which the cerebral cortex is derived (*23*). [At 12 to 13 weeks, VZ cells normally cease giving rise to the neurons in layers IV to VI and begin contributing to neurogenesis in layers II and III (*27*) (Fig. 1, schematic I).] Pregnancy was allowed to continue to the completion of most cortical neurogenesis at ~16 to 17 weeks gestation (Fig. 1, schematic II), when the fetuses were delivered by Cesarean section and their brains were processed for histological analysis (*28*) (Fig. 2). Distribution of donor human NSCs (hNSCs) in the monkey brains was monitored by immunocytochemical staining for the BrdU marker (Figs. 1 and 3) (*28*). To provide further independent confirmation of the cells' origin, we used, in parallel, antibodies against additional donor-specific markers, including the human-specific nuclear mitotic antigen (NuMA) as well as other species-specific tags (*28*). The phenotypes of these cells were characterized by immunocytochemistry (*28*) (Fig. 3).

Unilaterally injected hNSCs distributed themselves throughout both cerebral hemispheres symmetrically and at most levels of the neuraxis, settling in diverse widespread regions of the telencephalon, principally at the frontal and frontoparietal levels (Fig. 3). Although the individual hNSCs were clonally related, they appeared to segregate into two subpopulations (Fig. 3), as follows.

Cells in subpopulation 1 (red stars in Fig.

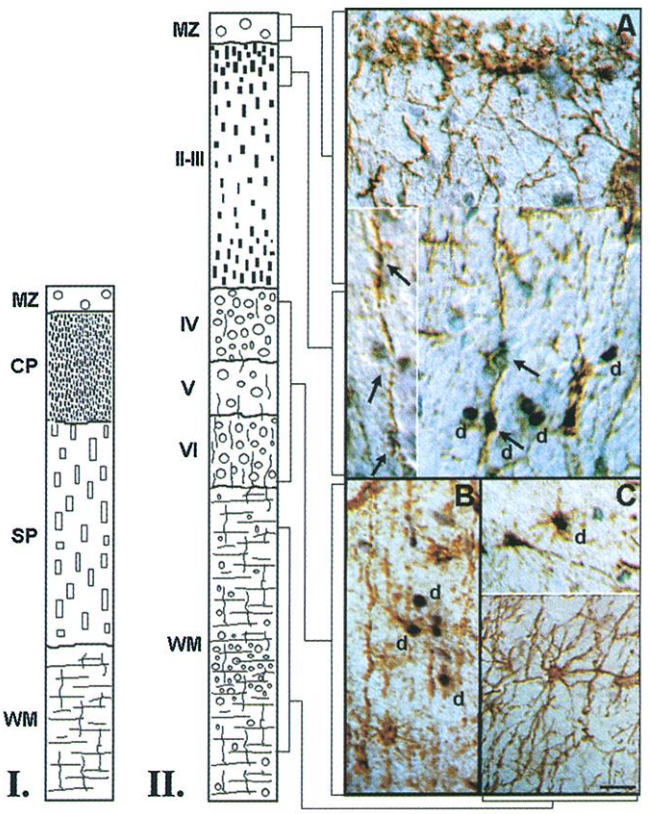


**Fig. 1.** Clonal hNSCs migrate from ventricular germinal zone (VZ) into developing neocortex. On the left are schematics of the developing monkey neopallium at the time of transplantation (I) [12 to 13 weeks postcoitum (pc)] and at the time of death (II) (16 to 17 weeks pc). See (*27*) and Web note 2 for brief description of primate neocortical development. Transplantation is described in (*23*). (**A** to **C**) Photomicrographs from selected locations spanning the neopallium. (Their location relative to the schematic is indicated by brackets.) (A) Injected into the left lateral ventricle and having integrated throughout the VZ, the hNSC-derived cells (d), identified by their BrdU immunoreactivity (black nuclei), migrated along the monkey's radial glial processes [visualized with an antibody to vimentin (brown)] through the neopallial wall to reach their temporally appropriate destination in the nascent superficial layers II and III (A), where they detached from the radial glia and took up residence as neurons (see Fig. 3 for closeups and characterization). Arrows indicate climbing cells (both donor- and host-derived) positioned along the processes of the vimentin-positive host radial glia. Some cells (**inset**) are pictured still attached to these fibers and in the process of migration. The photomicrographs in (B) and (C) show examples of immature, donor hNSC-derived (BrdU-positive black nuclei, d) astrocytes (brown vimentin-positive immunostain) intermixed with host-derived astrocytes in deeper cortical lamina, having differentiated as expected for that site and time. Abbreviations: MZ, marginal zone; CP, cortical plate; SP, subplate; WM, white matter; II to VI, cortical layers. Scale bar, 35 μm.

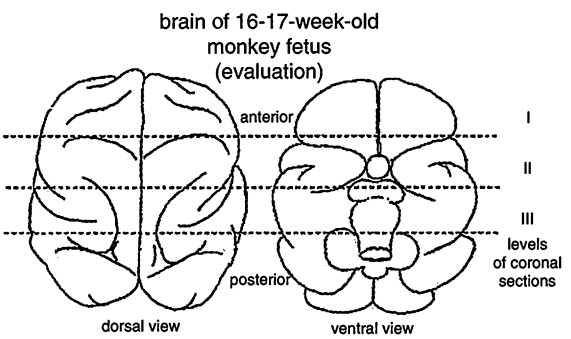


**Fig. 2.** Evaluation of engrafted monkey brains at the conclusion of neocortical development. Brains were retrieved as described in (*23*) and analyzed in three anterior-posterior segments (I to III), as illustrated. For histological methods, see (*28*).

[1]Departments of Pediatrics, Neurosurgery, and Neurology, Children's Hospital, Harvard Medical School, 248 Enders Building, 300 Longwood Avenue, Boston, MA 02115, USA. [2]Department of Medicine and Pharmacology and the Neuroscience Program, University of Colorado School of Medicine, 4200 East 9th Avenue, Denver, CO 80220, USA. [3]Department of Pediatrics, College of Medicine, Yonsei University, Seoul, Korea. [4]Department of Neurology, University of British Columbia, Koerner Pavilion, 211 Wesbrook Mall, Vancouver, BC, Canada V6T 2B5. [5]Department of Neurosurgery, Brigham and Women's Hospital, Harvard Medical School, LMRC, 221 Longwood Avenue, Boston, MA 02115, USA.

*These authors contributed equally to this work.
†To whom correspondence should be addressed at present address: Beth Israel Deaconess Medical Center, Department of Neurology, 855 Harvard Institute of Medicine, 77 Avenue Louis Pasteur, Boston, MA 02115, USA. E-mail: esnyder1@caregroup.harvard.edu or vouredni@caregroup.harvard.edu
‡Co-senior authors.

3) appeared to traverse great distances (~1.6 cm or ~1600 times a migrating cell body diameter) from the periventricular germinal zones along host radial glial processes (Fig. 1A) to terminate at developmentally and temporally appropriate cortical laminae and differentiate into several neuronal (Fig. 3, A to D) and glial (Fig. 3, E to G) cell types. Those hNSCs that migrated to the superficial neurogenic cortical layers II and III (Fig. 1A, schematic II) appropriately became neurons (Fig. 3A, arrow), identified by dual immunoreactivity to antibodies to NeuN, calbindin, and neurofilament (Fig. 3, B to D, arrows), intermixed with the monkey's own neurons (arrowheads). The majority of the hNSC-derived neurons were found in cortical layers II and III [which, at the time of transplant, profited from an intensive supply of newly formed neurons (*27*, *29*)]. Those hNSC-derived cells that stopped and integrated within the deeper cortical layers IV to VI differentiated appropriately into glial cells (Fig. 1, B and C, schematic II), identified by immunoreactivity to glial fibrillary acidic protein (GFAP) (for astrocytes) or to 2′,3′-cyclic nucleotide 3′-phosphohydrolase (CNPase) (for oligodendrocytes) (Fig. 3, E to G). [Glial cells of donor origin were also appropriately observed in the marginal zone (MZ, layer I) (Fig. 1, schematic II) and in subcortical regions. Some donor cells contributed also to the radial glial cell population.]

Cells in subpopulation 2 (blue dots in Fig. 3) were small, undifferentiated BrdU-positive cells lacking neuronal processes and were dispersed throughout the SVZ as single cells or small clusters intermingled with the germinal cells of the host (Fig. 3, H and I). When double-stained for cell type–specific antigens, these cells expressed vimentin (an immature progenitor/stem cell marker) (Fig. 3I and inset) but were negative for all other markers of differentiation. The majority of such undifferentiated hNSC-derived cells remained within the SVZ [none in the ependyma (*18*)]. The SVZ has been implicated in postnatal and adult homeostatic mechanisms

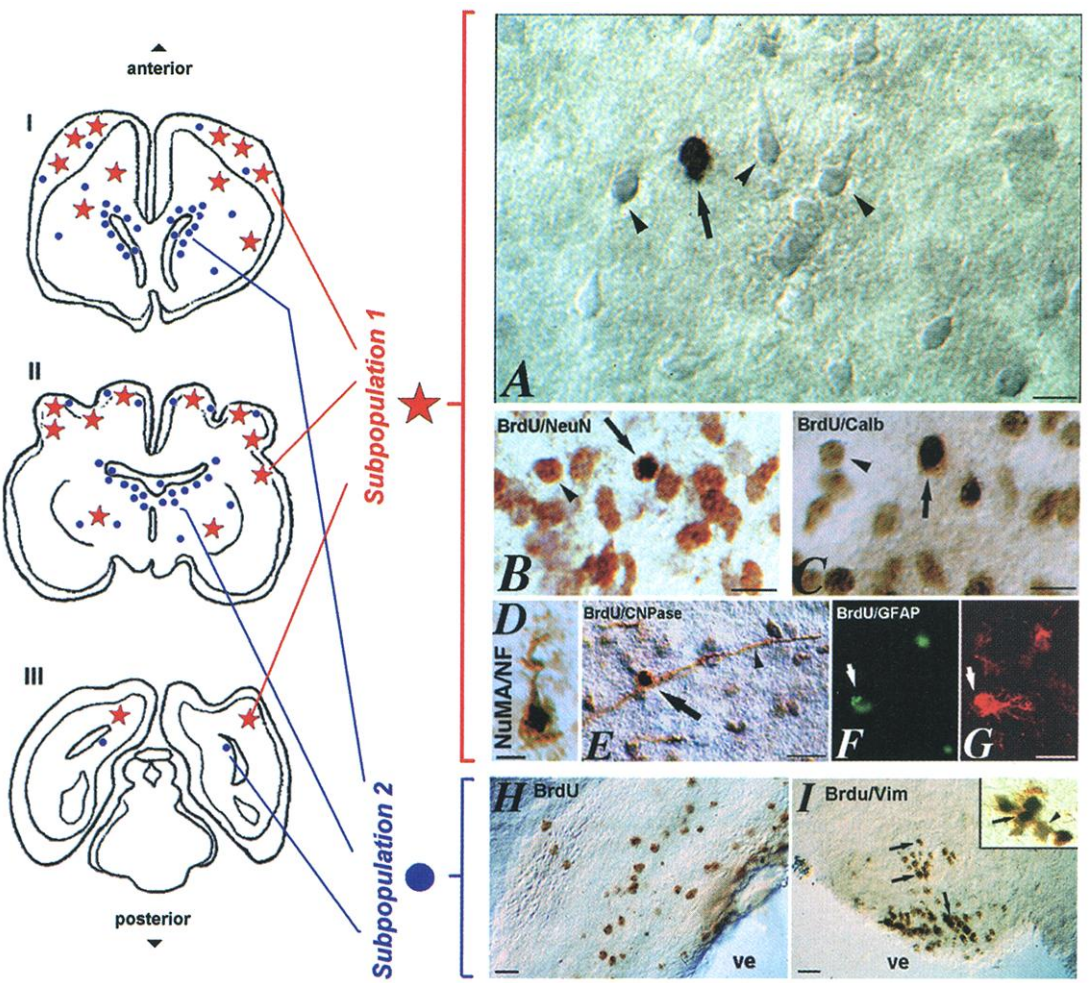


**Fig. 3.** Segregation of the fates of hNSCs and their progeny into two subpopulations in the brains of developing Old World monkeys. Schematics (**left**) and photomicrographs (**right**) illustrating the distribution and properties of clonal hNSC-derived cells. [Each coronal section in the schematic (I to III) corresponds to a coronal level (I to III) in Fig. 2.] hNSCs [labeled with BrdU and implanted as per (*23*)] dispersed throughout and integrated into the VZ. From there, clonally related hNSC-derived cells pursued one of two fates, as shown by immunocytochemical analysis (**A** to **I**) (*28*). Those donor cells that migrated outward from the VZ along radial glial fibers (as per Fig. 1) into the developing neocortex constituted one pool or subpopulation. The differentiated phenotypes of cells in this subpopulation 1 (red stars in the schematic) (particularly in layers II and III) are pictured in panels (A) to (G). (A) An hNSC-derived BrdU-positive cell (black nucleus, arrow)—likely a neuron according to its size, morphology, large nucleus, and location—is visualized (under Nomarski optics) intermingled with the monkey's own similar neurons (arrowheads) in neocortical layers II and III. The neuronal identity of such donor-derived cells is confirmed by immunocytochemical analysis in (B) to (D). (B, C, and E to G) High-power photomicrographs of human donor-derived cells integrated into the monkey cortex double-stained with antibodies against BrdU and cell type–specific markers: (B) NeuN and (C) calbindin for neurons (arrows, donor-derived cells; arrowheads, host-derived cells). (E) CNPase for oligodendroglia (arrow, BrdU-positive black nucleus in CNPase-positive brown cell; arrowhead indicates long process emanating from the soma). (F and G) GFAP for astroglia [antibody to Brd U revealed via fluorescein in (F); antibody to GFAP revealed via Texas Red in (G)]. The human origin of the cortical neurons is further independently confirmed in (D) where the human-specific nuclear marker NuMA (black nucleus) is colocalized in the same cell with neurofilament (NF) immunoreactivity (brown). Progeny from this same hNSC clone were also allocated to a second cellular pool—subpopulation 2 [blue dots in the schematic and pictured in (H) and (I) (arrows)]—that remained mainly confined to the SVZ and stained only for an immature neural marker [vimentin (brown) colocalized with BrdU (black nucleus) better visualized in inset (arrows); arrowhead indicates host vimentin-positive cell]. Some members of subpopulation 2 were identified within the developing neocortex (blue dots) intermixed with differentiated cells. (F) and (G) use immunofluorescence; the other immunostains use a DAB-based color reaction. The photomicrographs were taken from different animals as representative of all animals. ve, lateral cerebral ventricle; arrow, BrdU-positive donor-derived cell; arrowhead, BrdU-negative, host-derived cell except in (E). Scale bars, 30 μm [(A) to (C)]; 20 μm [(D) to (I)].

(*16*, *17*, *30*, *31*) and as an ongoing source of cortical neurons after overt cortical development has ceased (*32*–*34*). A small number of subpopulation 2 cells, however, were present within the striatum and cortex, intermixed with the differentiated cells (Fig. 3). These cells may provide a local resident pool for self-repair and plasticity and may represent the stemlike cells extracted by several investigators (*10*, *13*, *15*, *22*, *35*). [This observation favors the interpretation that such reported cells are not simply the result of dedifferentiation of committed progenitors, an artifact of experimental manipulation, as has occasionally been speculated (*10*, *11*)].

Our data provide a plausible dynamic for how multiple, disparate stem cell populations are generated as part of a single strategy of NSC allocation. The clonal progeny of a given NSC segregate to yield some differentiated cells for organogenesis (e.g., subpopulation 1) and other cells (e.g., subpopulation 2) for deposition in secondary germinal zones (e.g., the SVZ) as a reservoir. The NSCs that have been isolated from adults are likely descendants of the same NSCs that contributed to embryonic and fetal CNS development and thus do not represent a unique pool. In this view, ongoing lifelong self-repair and plasticity are a fundamental developmental program set in place during early stages of brain organogenesis. Grafted hNSCs appear to become integrated into the morphogenetic program of the developing primate host brain (Figs. 1 and 3) (*36*). Although it was not technically possible in these monkeys to quantify rigorously the percentage of grafted cells that survived, the histological images show that a large number of donor-derived cells were present bilaterally in all recipients (*37*, *38*). That hNSCs can migrate through the large expanse of the primate cerebrum, not merely through the much smaller rodent brain (*5*–*7*), suggests that migration may be a fundamental stem cell property limited only by available terrain (large or small). In rodents, NSCs have been shown to be well-suited for transplant-based approaches to gene therapy and/or cell replacement in diseases characterized by extensive or global abnormalities (*39*). Our results suggest that this approach may similarly be feasible in large primates and possibly humans.

### References and Notes


1. E. Gussoni *et al.*, *Nature* **401**, 390 (1999).
2. M. F. Pittenger *et al.*, *Science* **284**, 143 (1999).
3. A. L. Vescovi *et al.*, *Exp. Neurol.* **156**, 71 (1999).
4. C. N. Svendsen *et al.*, *Exp. Neurol.* **148**, 135 (1997).
5. J. D. Flax *et al.*, *Nature Biotechnol.* **16**, 1033 (1998).
6. N. Uchida *et al.*, *Proc. Natl. Acad. Sci. U.S.A.* **97**, 14720 (2000).
7. F. J. Rubio, C. Bueno, A. Villa, B. Navarro, A. Martinez-Serrano, *Mol. Cell Neurosci.* **16**, 1 (2000).
8. P. S. Eriksson *et al.*, *Nature Med.* **4**, 1313 (1998).
9. N. S. Roy *et al.*, *Nature Med.* **6**, 271 (2000).
10. T. D. Palmer, E. A. Markakis, A. R. Willhoite, F. Safar, F. H. Gage, *J. Neurosci.* **19**, 8487 (1999).
11. T. Kondo, M. Raff, *Science* **289**, 1754 (2000).
12. E. Y. Snyder *et al.*, *Cell* **68**, 33 (1992).
13. B. A. Reynolds, S. Weiss, *Science* **255**, 1707 (1992).
14. O. Brustle *et al.*, *Nature Biotechnol.* **16**, 1040 (1998).
15. Q. Shen, X. Qian, A. Capela, S. Temple, *J. Neurobiol.* **36**, 162 (1998).
16. J. M. Garcia-Verdugo, F. Doetsch, H. Wichterle, D. A. Lim, A. Alvarez-Buylla, *J. Neurobiol.* **36**, 234 (1998).
17. C. M. Morshead, C. G. Craig, D. van der Kooy, *Development* **125**, 2251 (1998).
18. C. B. Johansson *et al.*, *Cell* **96**, 25 (1999).
19. P. J. Renfranz, M. G. Cunningham, R. D. McKay, *Cell* **66**, 713 (1991).
20. V. Tropepe *et al.*, *Science* **287**, 2032 (2000).
21. L. S. Shihabuddin, P. J. Horner, J. Ray, F. H. Gage, *J. Neurosci.* **20**, 8727 (2000).
22. D. M. Panchision *et al.*, *Genes Dev.* **15**, 2094 (2001).
23. See also Web note 1 (*24*). Cells from a stable, self-maintaining clone of hNSCs (clone H6), originally isolated from the VZ of a 15-week human fetal cadaver and generated, grown, and characterized as previously described (*5*), were preincubated in culture (at a density of $5 \times 10^5$ cells/ml) with BrdU (10 μM, Sigma) for 48 hours before implantation in order to be subsequently identifiable in vivo by their darkly stained BrdU-immunopositive nuclei. (The cells were derived from a human developmental stage more immature than that of the monkey recipients.) The hNSCs were then resuspended in phosphate-buffered saline (PBS) at $1.7 \times 10^7$ cells/ml (as previously described) (*5*). This allowed 60 to 70% of the cells to become BrdU-labeled in vitro without toxicity; the BrdU remains detectable in vivo for at least 5 to 10 cell divisions, beyond the number known to occur for stem cells in vivo. Three pregnant bonnet monkeys were anesthetized with acepromazine [0.5 mg/kg intramuscularly (IM)], ketamine (10 mg/kg IM), and atropine sulfate (0.4 mg/kg IM). Ketamine (0.02 mg/kg IM) was administered every 15 min during the grafting procedure. The skin of the mother's abdomen was shaved, washed with betadine/alcohol, and locally anesthetized with lidocaine. The fetal head was palpated through the abdominal wall and visualized by ultrasound. Under ultrasound guidance, an 18G spinal needle attached to a 10-ml syringe was inserted through the abdominal and uterine walls into the left lateral ventricle of the fetal brain. 1.53 to $2.21 \times 10^7$ hNSCs were injected in a volume of 0.9 to 1.3 ml over a period of 2 min. Implantation into the cerebral ventricle allows reliable and uniform access of the hNSCs to the VZ into which they integrate avidly [(*5*, *14*); K. Campbell *et al.*, *Neuron* **15**, 1259 (1995); H. D. Lacorazza *et al.*, *Nature Med.* **4**, 424 (1996); C. A. Walsh, C. L. Cepko, *Nature* **362**, 632 (1993); C. P. Austin, C. L. Cepko, *Development* **110**, 713 (1990)]. The procedure took ~30 min/animal. Antibiotics were given IM to the mothers daily for 3 days. Two of the pregnant monkeys also received cyclosporin (Sandoz) [15 mg/kg intravenously (IV)]; cyclosporin treatment continued at the same daily dose per orum (PO) throughout the survival period. The third mother received no immunosuppression. After the procedure, animals were housed individually in their cages and maintained on a regular feeding schedule. No pain, bruising, inflammation, or behavioral changes were observed and pregnancies continued normally. One month after engraftment, each of the pregnant monkeys was anesthetized and placed on an isoflurane ventilator. The abdomen was antiseptically prepared, and the fetus was removed by Cesarean section and killed by a pentobarbital overdose. All surgeries were successful and the mothers returned to their breeding groups after 3 weeks of recovery in individual housing. The removed fetuses were perfused with chilled heparinized saline (240 ml) followed by 4% paraformaldehyde (240 ml). Each brain was immersed in the fixative for an additional 5 hours at 4°C. The tissue was then cryoprotected in 30% sucrose in PBS and kept at 4°C until further processing. For histological analysis, the brains were partitioned into three coronal anterior-posterior segments (I to III) as illustrated in Fig. 2. At each level, 25 to 30 serial 35-μm coronal sections were cut on a freezing microtome. Slides were kept at 4°C or, for longer storage, at −20°C. For each individual immunostaining, three sections from each level were analyzed. For histological methods, see (*28*).
24. Web material is available at www.sciencemag.org/cgi/content/full/1060580/DC1.
25. The basic patterns of cell genesis, migration, and differentiation, initially worked out in rodents [S. A. Bayer *et al.*, *Neuroimage* **1**, 296 (1994); P. Rakic, *Proc. Natl. Acad. Sci. U.S.A.* **92**, 11323 (1995)], are found also, although on a much prolonged time schedule, in primates [P. Rakic, *J. Comp Neurol.* **145**, 61 (1972); B. Granger *et al.*, *J. Comp. Neurol.* **360**, 363 (1995); M. J. Donoghue, P Rakic, *Cerebr. Cortex* **9**, 586 (1999); P. S. Goldman-Rakic, *Neurosci. Res. Program Bull.* **20**, 520 (1982)]. NSCs of human derivation appear to have many properties similar to those isolated from rodents but have been assessed only within the context of the rodent brain (*3*–*7*). The smaller, less complex rodent brain might impose a set of behaviors on NSCs that might not be predictive of their fate in a primate brain. Not only are the physical dimensions very different in rodents compared with most primates, but the temporal scale for neocortical genesis spans several weeks to months in Old World monkeys and humans, compared with a few days in rodents. For example, would human NSCs, which can travel the expanse of the rodent brain, actually migrate from the periventricular germinal zones to the relatively distant and more expansive cerebral cortical plate of the much larger primate brain?
26. Although neurogenesis has not previously been studied specifically in bonnet monkeys (*Macaca radiata*), data are available in the closely related rhesus monkey (*Macaca rhesus*) [I. Kostovic, P. Rakic, *J. Comp. Neurol.* **297**, 441 (1990); D. R. Kornack, P. Rakic, *Proc. Natl. Acad. Sci. U.S.A.* **95**, 1242 (1998)]. Monkeys of the two species have almost identical gestation periods of ~22 to 23 weeks and are similar in size at birth and in adulthood. Hence, we extrapolated from data in *M. rhesus* to times and location of cerebral neurogenesis in *M. radiata*.
27. See also Web note 2 (*24*). At the time of transplantation, the cerebral cortex consists of a cortical plate (CP) and subplate (Fig. 1, schematic I). The layers characteristic of the mature neocortex (Fig. 1, schematic II) have not yet appeared. Young postmitotic neurons already in the CP will differentiate to form the relatively sparse neuronal population of layer I (marginal zone) and the numerous neurons of the deeper cortical layers IV to VI. Neurons destined for superficial cortical layers II and III at the time of engraftment are just being generated and will migrate out from the VZ during the postgrafting survival period of 1 month, mainly along the leading processes of radial glia. Also generated during the 1-month survival period are glial cells destined to reside in the subcortex and deeper cortical layers; most glial cells destined for the superficial cortical layers will not be generated until after the time of death. [For review, see (*25*, *26*, *36*).]
28. Sections were brought to room temperature (RT) and processed for BrdU immunostaining as described previously [J. Ourednik *et al.*, *J. Comp. Neurol.* **395**, 91 (1998)]. After extensive washes in PBS, sections were hydrolyzed with 2 M HCl and incubated for 60 min at RT with a rat monoclonal antibody to BrdU (Sera-Lab). The sections were then washed and incubated for 75 min at RT with a biotinylated antibody to rat immunoglobulin (Vector). The subsequent color reaction was developed according to the ABC Vectastain protocol (Vector) with Ni/Co enhancement. Sections were dehydrated, mounted in Entellan (Merck), and examined with a Nikon microscope equipped with Nomarski optics. Parallel staining with multiple human-specific monoclonal antibodies to NuMA (Chemicon, 1:40 and Calbiochem, 1:400), human ribonuclear protein (Chemicon, 1:20), and the human EGF receptor (Upstate Biotech, 1:100) was performed according to standard protocols also with the Vectastain kit. Double-immunostaining was carried out with antibodies to BrdU or NuMA and the following cell type–specific markers: monoclonal antibody to NeuN (gift from R. Mullen), antibody to calbindin (Chemicon), antibody to NF (Roche), antibody to CNPase (Chemicon), and antibody to vimentin (Chemicon). The procedure was a differential

diaminobenzidine (DAB)–based reaction with Ni/Co-enhanced antibody to BrdU as described above, combined with a standard, nonenhanced reaction revealing the cell type. The double-staining for donor-derived astrocytes (colocalization of BrdU and GFAP) followed a similar protocol with a rabbit polyclonal antibody to GFAP (Daco) but with the two secondary antibodies (Vector Labs) coupled to different fluorochromes: fluorescein to reveal BrdU and Texas Red for GFAP. As noted above, we used multiple independent markers to show unambiguously donor derivation of the examined cells; the labeling distribution for each of the markers was the same.

29. G. D. Frantz, S. K. McConnell, *Neuron* **17**, 55 (1996).
30. S. A. Goldman, M. B. Luskin, *Trends Neurosci.* **21**, 107 (1998).
31. A. Kakita, J. E. Goldman, *Neuron* **23**, 461 (1999).
32. E. Gould, A. J. Reeves, M. S. Graziano, C. G. Gross, *Science* **286**, 548 (1999).
33. S. S. Magavi, B. R. Leavitt, J. D. Macklis, *Nature* **405**, 951 (2000).
34. K. I. Park, E. Y. Snyder, *Soc. Neurosci. Abstr.* **24**, 1310 (1998).
35. M. F. Mehler, S. Gokhan, *Brain Pathol.* **9**, 515 (1999).
36. R. L. Sidman, P. Rakic, in *Histology and Histopathology of the Nervous System*, W. Haymaker, R. D. Adams, Eds. (Thomas, Springfield, MA, 1982), pp. 3–145.
37. An evaluation of surviving grafted cells in all three animals revealed ~150 to 200 cells per 35-μm coronal section in the most densely engrafted areas (usually at level I; see Fig. 2) and ~10 cells per section in the more sparsely engrafted regions. Whether this distribution reflects a genuine anterior-posterior developmental gradient or simply a stochastic distribution of cells or the product of transplantation technique cannot yet be determined. An estimate of ~$10^5$ hNSC-derived cells were detectable per monkey brain. hNSCs segregated in about a 3:7 ratio proportion between subpopulation 1 and subpopulation 2, respectively. Of subpopulation 1 cells in the cortex, 7 to 8% were neurons, 80% were astrocytes, and 12% were oligodendrocytes; the neurons were almost invariantly in the appropriate laminae II and III.
38. Two of the three pregnant monkeys received cyclosporin, as described in (*23*). No histological evidence of inflammatory reaction or of cell rejection was seen in any of the three specimens. Experiments of longer duration and with grafting at more mature ages will be necessary to test whether rejection might ultimately have occurred; however, there is the suggestion that, at least at certain stages, an immunotolerance for NSCs might exist.
39. V. Ourednik, J. Ourednik, K. I. Park, E. Y. Snyder, *Clin. Genet.* **56**, 267 (1999).
40. Funded by National Institute of Neurological Disorders and Stroke, March of Dimes, Project ALS, A-T Children's Project, Mental Illness Research Association, Kingspoint Richmond Foundation, Conavan Research Fund, Hunter's Hope, International Organization for Glutaric Acidemia, a Mental Retardation Research Center Grant to Children's Hospital, Program to End Parkinson's Disease, and Parkinson's Action Network.

9 March 2001; accepted 16 July 2001
Published online 26 July 2001;
10.1126/science.1060580
Include this information when citing this paper.

# Allele-Specific Receptor-Ligand Interactions in *Brassica* Self-Incompatibility

**Aardra Kachroo, Christel R. Schopfer,* Mikhail E. Nasrallah, June B. Nasrallah†**

**Genetic self-incompatibility in *Brassica* is determined by alleles of the transmembrane serine-threonine kinase SRK, which functions in the stigma epidermis, and of the cysteine-rich peptide SCR, which functions in pollen. Using tagged versions of SRK and SCR as well as endogenous stigma and pollen proteins, we show that SCR binds the SRK ectodomain and that this binding is allele specific. Thus, SRK and SCR function as a receptor-ligand pair in the recognition of self pollen. Specificity in the self-incompatibility response derives from allele-specific formation of SRK-SCR complexes at the pollen-stigma interface.**

In self-incompatible *Brassica* plants, self-pollinations and crosses between genetically related individuals are nonproductive because self-related pollen grains are inhibited upon contact with the epidermal cells of the stigma, a structure that caps the female reproductive organ. Specificity in this self-incompatibility (SI) response is determined by haplotypes of the polymorphic *S* locus. The self-recognition molecules encoded by this locus include the single-pass transmembrane receptor–like serine-threonine kinase SRK, which functions in the stigma epidermis (*1–3*) and becomes phosphorylated upon self-pollination (*4*), and the cysteine-rich peptide SCR, which functions in pollen (*5*, *6*). These two molecules are highly polymorphic, with allelic forms of SRK and SCR exhibiting 10 to 30% and >60% divergence, respectively (*1*, *5–8*). Views of SRK as a ligand-activated receptor kinase and SCR as its ligand are consistent with the predicted molecular properties of these molecules and the rapidity of the SI response (*1*, *9*). The SCR peptide is localized on the surface of pollen grains (*10*). During self-pollination, SCR is predicted to bind the receptor domain of its cognate SRK, thereby triggering an intracellular phosphorylation cascade that leads to inhibition of pollen hydration and germination. Specificity in the SI response is thought to result from haplotype-specific activation of SRK by SCR. Here, we describe experiments that demonstrate a physical and haplotype-specific interaction between SCR and the ectodomain of SRK.

To investigate the SRK-SCR interaction, we generated tagged versions of the two proteins. Recombinant $eSRK_6$, consisting of the ectodomain of $SRK_6$ (from the $S_6$ haplotype) and carrying a COOH-terminal FLAG epitope tag, was expressed as a soluble secreted glycoprotein in *Nicotiana benthamiana* leaves using the potato virus X expression system (*11*). $eSRK_6$ protein migrated as two molecular mass forms of ~63 and 70 kD on SDS–polyacrylamide gel electrophoresis (SDS-PAGE), which presumably reflect differential glycosylation of $eSRK_6$-FLAG in *Nicotiana* leaves. $SCR_6$ and $SCR_{13}$ (the SCRs of the $S_6$ and $S_{13}$ haplotypes, respectively) were expressed in bacteria as secreted periplasmic proteins carrying a COOH-terminal myc-$His_6$ tag (*11*). They exhibited expected masses of ~8 and 9 kD, respectively, but they migrated as doublets, possibly due to inefficient cleavage of the periplasmic signal peptide in bacteria.

Recombinant SCR-myc-$His_6$ was shown to be biologically active in pollination bioassays (*12*). Pretreatment of stigmas with purified "self" SCR protein (i.e., $S_6S_6$ stigmas with $SCR_6$-myc-$His_6$ or $S_{13}S_{13}$ stigmas with $SCR_{13}$-myc-$His_6$) mixed with pollen-coat protein carrier (*12*) caused these stigmas to inhibit the germination of normally compati-

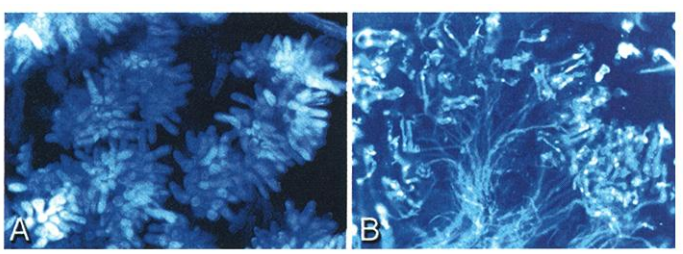


**Fig. 1.** Effect of purified recombinant SCR protein on cross-pollen tube development. $S_6S_6$ stigmas (**A**) and $S_2S_2$ stigmas (**B**) were treated with $SCR_6$-myc-$His_6$ and pollinated with $S_{13}$ pollen (*12*). Addition of "self" $SCR_6$-myc-$His_6$ triggers inhibition of normally compatible $S_{13}$ pollen on $S_6S_6$ but not on $S_2S_2$ stigmas.

Department of Plant Biology, Cornell University, Ithaca, NY 14853, USA.

*Present Address: SunGene GmbH, Correnssstrasse 3, D-06466, Gatersleben, Germany.
†To whom correspondence should be addressed. E-mail: jnb2@cornell.edu